IEEE Access
Multidisciplinary | Rapid Review | Open Access Journal

Received February 27, 2019, accepted March 18, 2019, date of publication March 25, 2019, date of current version April 13, 2019.

Digital Object Identifier 10.1109/ACCESS.2019.2907136

High Resolution Direct Detection and Position Determination of Sources With Intermittent Emission

KEGANG HAO, (Student Member, IEEE), AND QUN WAN, (Member, IEEE)
School of Information and Communication Engineering, University of Electronic Science and Technology of China, Chengduis 611731, China

Corresponding author: Qun Wan (wanqun@uestc.edu.cn)

This work was supported in part by the National Natural Science Foundation of China (NSFC) under Grant 61771108, in part by the National Science and Technology Major Project under Grant 2016ZX03001022, and in part by the Foundation of Sichuan Science and Technology Project under Grant 18ZDYF0990 and Grant 19ZDYF0487.

ABSTRACT This paper presents our research findings on the direct detection and position determination (DDPD) problem, which is to estimate the positions and the total number of multiple sources with intermittent emission, using the received signals intercepted by a moving antenna array at multiple observation slots. We combine the direct position determination (DPD) concept and the Minimum Variance Distortionless Response (MVDR) criterion to solve the DDPD problem without the prior knowledge of the effective number of sources (the number of sources at every observation slot). We find out that the parallel combination of the MVDR spectrum in the cost function results in its own sensitivity to the missing emission, which makes the location estimator bias. Therefore, we use the K-means clustering algorithm to identify the sources with intermittent emission and their emitting slots adaptively, based on the MVDR spectrum values over all observation slots. Then, we use the spectrum values of the identified emitting slots to reconstruct the MVDR spectrum. Finally, we find the peaks of the reconstructed MVDR spectrum, which are corresponding to the source positions. The results of the simulations demonstrate that the proposed method gets asymptotic performance with the signal to noise ratio (SNR), both in the aspects of the root mean square error (RMSE) and the bias error, and high resolution as a generalized MVDR based method.

INDEX TERMS Direct position determination, passive localization, array processing, maximum likelihood, minimum variance distortionless response (MVDR).

I. INTRODUCTION

The localization of sources emitting electromagnetic or acoustic energy has been studied for several decades and applied in many engineering applications such as the sound processor of Artificial Cochlea, Location-Based Services(LBS) in communication systems, wild-life tracking, earthquake monitoring and targets detection in military. The classical localization methods are two-step processing [1]–[5]. Firstly, intermediate parameters that rely on the locations of the sources are estimated from the measurements of different origin (these parameters are usually the angle of arrival (AOA), time difference of arrival (TDOA), Doppler frequency shift (DFS) or received signal strength (RSS)). And then the estimated parameters are used to estimate the locations of sources based on Maximum likelihood (ML) criterion or others.

The DPD approach has recently been proposed [6], [7] as a single-step ML localization technique. The DPD method estimates the parameters of interest by minimizing a single cost function into which all received data batches enter jointly. This can be viewed as searching for the source location that best explains the collected data. From the view of information theory, the two-step method is more likely to damage the localization information during the estimation of intermediate parameters that DPD method avoids. This is the reason why DPD method outperforms the two-step method at low SNR. Furthermore, an additional data association step to partition the intermediate estimated parameters into sets belonging to the same source is required in multiple sources scenario, which is avoided inherently in DPD method. Multiple hypotheses tracking (MHT) is generally accepted as

The associate editor coordinating the review of this manuscript and approving it for publication was Yue Ivan Wu.

the preferred method for solving the measurement-to-track association problem [8]. However, in multiple sources scenario, the exact ML estimator can be derived but it requires a multi-dimensional search which is usually impractical. The DPD method is no longer equivalent to the ML estimator.

The DPD concept was extended to the case of multiple sources with intermittent emission [9] and the authors Oispuu M et al used the alternating projection (AP) technique [10] to solve the high-dimensional ML optimization by a series of low-dimensional optimizations. Whereas the considered DPD approach requires knowledge of the total number of sources, but in practice this number is unknown. Oispuu M et al proposed an iterative method to determinate the positions and the total number of sources alternately. This DDPD method is based on the fact that the optima of the ML-DPD object function are χ^2- distributed and requires the knowledge of the effective number of sources, which implies that the DDPD method is also dependent on the model order determination and likely to suffer from the error of model order determination.

Another alternative estimator for the ML estimator of the DDPD problem is MVDR estimator which doesn't need the prior knowledge of the number of sources (the model order). It was originally proposed by Capon [11] for frequency-wavenumber power spectral density analysis, but has since been used extensively as a high resolution method. Recently, the MVDR concept and DPD are combined to create a high resolution estimator that can localize multiple dense sources that transmit unknown narrowband signals [12]–[14]. In fact, Oispuu M et al had already introduced the MVDR concept to localize multiple sources with intermittent emission directly [9]. Unfortunately, the location spectrum based on the Capon type object function is distorted by the missing emission of sources and the MVDR estimator has large bias error even at high SNR.

In this paper, we find out why the original MVDR spectrum is sensitive to the missing emission. The reason is that the Capon type object function combines the received power from a given position in every emitting slots in a way that resembles the combination of parallel resistors. In order to improve the robustness of the location MVDR-spectrum under the intermittent emission condition, we proposed to identify the emitting/non-emitting slots of a source adaptively using classical K-means clustering algorithm and then modify the position MVDR-spectrum by eliminating the power value of the non-emitting slots. The simulation results indicate that the modified position MVDR-spectrum gets high resolution and asymptotic performance with SNR.

The rest of this paper is organized as follow: Section II formulates the signal model and the DDPD problem. The original MVDR spectrum is discussed in the first subsection of Section III to show its limitation. The modified MVDR spectrum is proposed in the next subsection. Simulations are outlined in Section IV and Section V concludes this paper.

Following the convention, this paper uses unified symbols and notations defined in Table 1.

TABLE 1. Notations.

Symbol	Description
$\boldsymbol{a}$, $\boldsymbol{A}$	vector and matrix
$[\cdot]^T$, $[\cdot]^H$	transpose and conjugate transpose
$\circ$	hadamard product
$\Vert\cdot\Vert_2$	Euclidean norm
$\text{blkdiag}[(*), \cdots, (\bullet)]$	block diagonal matrix with diagonal blocks $(*), \cdots, (\bullet)$
$\boldsymbol{I}_N$	identity matrix of size $N \times N$
$\text{descend}[\cdot]$	output the vector with elements in descending order

II. PROBLEM FORMULATION

We consider a scenario where there are Q fixed sources with intermittent emission (i.e. emitting signals with probabilities at every observation slot) located at $\boldsymbol{p}_q = (x_q, y_q, z_q)^T$, $q = 1, \ldots, Q$ and an antenna array composed of M elements, mounted on a moving platform. The array is assumed to receive narrowband signals (i.e. the receiving bandwidth is much smaller than the reciprocal of the time delay across the array) with wavelengths centered around a common wavelength λ. The array moves along an arbitrary but known trajectory. During the movement of the array, K data batches are collected at the sensor positions $\boldsymbol{u}_k$, $k = 1, \ldots, K$ with a sufficiently high data rate. The signals of each source is only contained in $K_q \leq K$ data batches since the sources emit intermittently. The scenario is assumed to be stationary during one batch and non-stationary from batch to batch. The schematic of the scenario are illuminated in Fig.1.

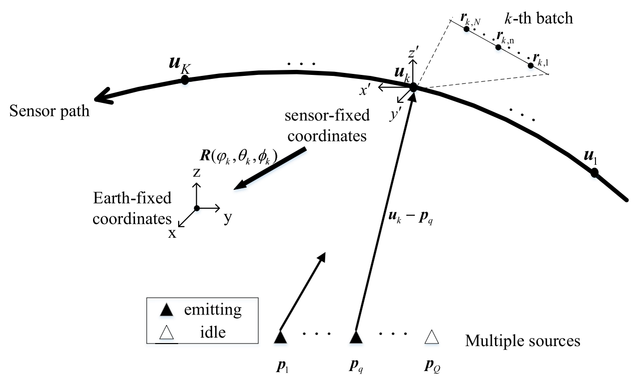

FIGURE 1. The schematic of the scenario.

Given the output of the array be sampled sequentially at N different and mutually exclusive snapshots and the sensor's displacement can be negligible during every observation. The n-th sample of the k-th received data batch can be expressed as

$$\boldsymbol{r}_{k,n} = \sum_{q=1}^{Q} \boldsymbol{a}_k(\boldsymbol{p}_q) b_{k,q} s_{k,n,q} + \boldsymbol{w}_{k,n}, \quad n = 1, \ldots, N \qquad (1)$$

where $\boldsymbol{r}_{k,n} \in \mathbb{C}^{M\times 1}$ denotes the complex envelopes formed from the signals received by the array elements. $b_{k,q}$ is a binary variable corresponding to the case where the q-th source is emitting or non-emitting at k-th observation slot. The emitting probability of the q-th source denoted by $P_q = P(b_{k,q} = 1)$ is assumed constant over all observation slots [9]. Note that the assumption is used to simplify the theoretical analysis and is unnecessary in practical application. $s_{k,n,q}$ is the n-th sample of the complex envelope of the q-th source signal measured at k-th slot if it emits, i.e. $b_{k,q} = 1$. $\boldsymbol{w}_{k,n} \in \mathbb{C}^{M\times 1}$ is a white, zero-mean, complex Gaussian noise with variance $\sigma_w^2 \boldsymbol{I}_M$ known. $\boldsymbol{a}_k(\boldsymbol{p}_q) \in \mathbb{C}^{M\times 1}$ is the array transfer vector which is considered quasi static during each observation, i.e. it doesn't rely on the index of samples n.

The array transfer vector expresses the complex response at the k-th observation slot to the planar wavefront arriving from the q-th source. We assume that the antenna array is perfectly calibrated so the array transfer vector can be parameterized by the source positions:

$$\boldsymbol{a}_k(\boldsymbol{p}_q) = (e^{j\boldsymbol{k}_k^T(\boldsymbol{p}_q)\boldsymbol{d}_1}, \ldots, e^{j\boldsymbol{k}_k^T(\boldsymbol{p}_q)\boldsymbol{d}_M})^T \tag{2}$$

It can be seen that the array transfer vector depends on the wavenumber vector

$$\boldsymbol{k}_k(\boldsymbol{p}_q) = \frac{2\pi}{\lambda} \frac{\boldsymbol{u}_k - \boldsymbol{p}_q}{\|\boldsymbol{u}_k - \boldsymbol{p}_q\|_2} \tag{3}$$

and $\boldsymbol{d}_m$ denotes the position of the m-th element relative to the sensor position $\boldsymbol{u}_k$ in earth-fixed coordinates.[1]

In practice, as the attitude of the sensor will change from observation to observation, the relative position vector $\boldsymbol{d}_m(k)$ varied with time reads

$$\boldsymbol{d}_m(k) = \boldsymbol{R}(\psi_k, \theta_k, \phi_k)\boldsymbol{d}'_m \tag{4}$$

where $\boldsymbol{d}'_m$ is the position of the m-th element in sensor-fixed coordinates,[2] which is constant once the array shape and the sensor-fixed coordinates is confirmed. The orientation of the sensor-fixed coordinates system (i.e. the attitude of the sensor) is given by the attitude (pitch,azimuth,roll) angles $(\psi_k, \theta_k, \phi_k)$ in earth-fixed coordinates, which a suitable rotation matrix $\boldsymbol{R}(\psi_k, \theta_k, \phi_k)$ (common in Navigation Technique literatures) is based on.

For the sake of simplicity, we assume that the antenna attitude does not change with time, i.e. the orientation of the sensor-fixed coordinates system is fixed over all observation slots $\boldsymbol{d}_m(k) = \boldsymbol{d}_m, k = 1, \ldots, K$.

The received data batches depend on the array transfer vectors which rely on the desired source positions. Thus, our DDPD problem is stated as follows: Estimate positions and the number of all sources $\{\boldsymbol{p}_q\}_{q=1}^Q$ from all received data batches $\{\{\boldsymbol{r}_{k,n}\}_{n=1}^N\}_{k=1}^K$ without the prior knowledge of the effective number of sources.

[1] A coordinate system whose origin is fixed on earth. The positions of all sources and receivers are denoted in it.

[2] A coordinate system which is fixed on the array. In practice, the positions of array elements are usually denoted in it, which have to be transformed into the earth-fixed coordinates.

III. THE ROBUST MVDR BASED DDPD METHOD

A. THE ORIGINAL MVDR SPECTRUM

The MVDR filter is used for adaptive beam forming and targets detection in parameter domain [15]. Recent researches [12]–[14] combine the concept DPD and MVDR criterion to get a high resolution DPD method. Besides, the time-varying interference caused by the intermittent emission can be suppressed by MVDR filter adaptively. Therefore, we choose the MVDR-based DPD method to get the high resolution position estimation of sources with intermittent emission. In order to build the MVDR optimization problem, the received signal data model in (1) need to be rewritten as

$$\boldsymbol{r}_{k,n} = \boldsymbol{a}_k(\boldsymbol{p}_q)b_{k,q}s_{k,n,q} + \boldsymbol{v}_{k,n} \tag{5}$$

where the first part of the summation is the received signal from the q-th source at position $\boldsymbol{p}_q$ and $\boldsymbol{v}_{k,n}$ contains the interference (the received signals from the rest of sources) and the noise.

As a consequence, for a location hypothesis $\boldsymbol{p}$, the coefficients of the traditional MVDR filter is given by

$$\begin{aligned} \boldsymbol{w}_k^*(\boldsymbol{p}) = arg \min_{\boldsymbol{w}_k} \boldsymbol{w}_k^H \hat{\boldsymbol{R}}_k \boldsymbol{w}_k \\ s.t.\ \boldsymbol{w}_k^H \boldsymbol{a}_k(\boldsymbol{p}) = 1 \qquad k = 1, \ldots, K \end{aligned} \tag{6}$$

where

$$\hat{\boldsymbol{R}}_k \triangleq \frac{1}{N}\sum_{n=1}^{N} \boldsymbol{r}_{k,n}\boldsymbol{r}_{k,n}^H \quad k = 1, \ldots, K \tag{7}$$

In order to acquire the distortionless signal waveform, the traditional MVDR filter processes each data batch respectively. Nonetheless, the distortionless constraints are unnecessary in our case, for we are not interested in the signal waveform but the source location. Therefore, we can relax the distortionless constraints to estimate the source location using all data batches, and to increase the degree of freedom used for noise and interference reduction.

We introduce the compact data model

$$\boldsymbol{r}_n = \boldsymbol{A}(\boldsymbol{p}_q)(\boldsymbol{b}_q \circ \boldsymbol{s}_{n,q}) + \boldsymbol{v}_n \tag{8}$$

by stacking the vectors on top and using a block-diagonal matrix

$$\begin{aligned} \boldsymbol{r}_n &= (\boldsymbol{r}_{1,n}^T, \ldots, \boldsymbol{r}_{K,n}^T)^T \in \mathbb{C}^{MK\times 1} \\ \boldsymbol{A}(\boldsymbol{p}_q) &= \text{blkdiag}[\boldsymbol{a}_1(\boldsymbol{p}_q), \ldots, \boldsymbol{a}_K(\boldsymbol{p}_q)] \in \mathbb{C}^{MK\times K} \\ \boldsymbol{b}_q &= (b_{1,q}, \ldots, b_{K,q})^T \in \{0,1\}^{K\times 1} \\ \boldsymbol{s}_{n,q} &= (s_{1,n,q}, \ldots, s_{K,n,q})^T \in \mathbb{C}^{K\times 1} \\ \boldsymbol{v}_n &= (\boldsymbol{v}_{1,n}^T, \ldots, \boldsymbol{v}_{K,n}^T)^T \in \mathbb{C}^{MK\times 1} \end{aligned}$$

For a location hypothesis $\boldsymbol{p}$, the MVDR optimization problem with the relaxed linear constraint is given as

$$\begin{aligned} \boldsymbol{w}^*(\boldsymbol{p}) = arg \min_{\boldsymbol{w}} \boldsymbol{w}^H \hat{\boldsymbol{R}} \boldsymbol{w} \\ s.t.\ \boldsymbol{w}^H \tilde{\boldsymbol{a}}(\boldsymbol{p}) = K \end{aligned} \tag{9}$$

where

$$\tilde{\boldsymbol{a}}(\boldsymbol{p}) \triangleq (\boldsymbol{a}_1^T(\boldsymbol{p}), \ldots, \boldsymbol{a}_K^T(\boldsymbol{p}))^T \in \mathbb{C}^{MK\times 1} \tag{10}$$

is composed of block-diagonal elements of $\boldsymbol{A}(\boldsymbol{p})$. And

$$\hat{\boldsymbol{R}} \triangleq \frac{1}{N}\sum_{n=1}^{N} \boldsymbol{r}_n\boldsymbol{r}_n^H = \text{blkdiag}[\hat{\boldsymbol{R}}_1, \ldots, \hat{\boldsymbol{R}}_K] \tag{11}$$

is the sample correlation matrix.

Now, we get an estimator of the source location

$$\hat{\boldsymbol{p}} = arg\max_{\boldsymbol{p}} J(\boldsymbol{p})$$
$$J(\boldsymbol{p}) \triangleq \boldsymbol{w}^{*H}(\boldsymbol{p})\hat{\boldsymbol{R}}\boldsymbol{w}^*(\boldsymbol{p}) \tag{12}$$

where $J(\boldsymbol{p})$ is the total output energy of the optimal MVDR filter.

Equation (9) describes minimization of a quadratic function under a linear constraint, and can be solved using the complex gradient operator [16]. The solution is given by

$$\boldsymbol{w}^*(\boldsymbol{p}) = K\frac{\hat{\boldsymbol{R}}^{-1}\tilde{\boldsymbol{a}}(\boldsymbol{p})}{\tilde{\boldsymbol{a}}^H(\boldsymbol{p})\hat{\boldsymbol{R}}^{-1}\tilde{\boldsymbol{a}}(\boldsymbol{p})} \tag{13}$$

Substituting (13) into (12) and ignoring the constant factor, we get the original location MVDR spectrum,

$$J(\boldsymbol{p}) = \frac{1}{\tilde{\boldsymbol{a}}^H(\boldsymbol{p})\hat{\boldsymbol{R}}^{-1}\tilde{\boldsymbol{a}}(\boldsymbol{p})} \tag{14}$$

The optimal weight vector $\boldsymbol{w}^*(\boldsymbol{p})$ in (9) minimizes the total output energy over K observation slots except that from the source at location $\boldsymbol{p}$, if it emits. So the peaks of the object function $J(\boldsymbol{p})$ for the area of interest will appear at all sources positions $\boldsymbol{p}_q$, $q = 1, \ldots, Q$. These spectrum peaks are usually selected using Constant-False-Alarm-Rate (CFAR) method.

B. THE MODIFIED MVDR SPECTRUM

According to the independence between observation slots, we get

$$\hat{\boldsymbol{R}}^{-1} = \text{blkdiag}[\hat{\boldsymbol{R}}_1^{-1}, \ldots, \hat{\boldsymbol{R}}_K^{-1}] \tag{15}$$

Substituting (10) and (15) into (14), we get

$$J(\boldsymbol{p}) = \frac{1}{\sum_{k=1}^{K}\boldsymbol{a}_k^H(\boldsymbol{p})\hat{\boldsymbol{R}}_k^{-1}\boldsymbol{a}_k(\boldsymbol{p})} \tag{16}$$

The expression (16) presents the combination of K MVDR-spectrums $\{J_k(\boldsymbol{p}) = [\boldsymbol{a}_k^H(\boldsymbol{p})\hat{\boldsymbol{R}}_k^{-1}\boldsymbol{a}_k(\boldsymbol{p})]^{-1}\}_{k=1}^K$ in a way that resembles the combination of K parallel resistors,

$$J(\boldsymbol{p}) = \frac{1}{\sum_{k=1}^{K} J_k^{-1}(\boldsymbol{p})} \tag{17}$$

It can be seen that the objective function (17) is sensitive to noise, i.e. the function value becomes very small as long as one of the K MVDR-spectrum values is corresponding to the noise energy and very small.

As a result of the sensitivity to noise in (17), the total received energy from the q-th source over all observation slots $J(\boldsymbol{p}_q)$ is disturbed by those much smaller energy values $J_{k'}(\boldsymbol{p}_q)$. These smaller energy values are corresponding to the observation slots in which the signals from the q-th source are absent (i.e. $b_{k',q} = 0$). To be more specific, the much smaller energy value $J_{k'}(\boldsymbol{p}_q)$ is at the level of noise since the q-th source doesn't emit at the k-th slot. The object function value $J(\boldsymbol{p}_q)$ will almost arrive at the level of noise even though other $J_k(\boldsymbol{p}_q)$, $k \neq k'$ are much larger (the q-th source emits at the k-th slot (i.e. $b_{k,q} = 1$)). This means that the information about the q-th source location in observation slots which contain the signals (i.e. the larger $J_i(\boldsymbol{p}_q)$) can not be used sufficiently. Thus the performance of the original location MVDR spectrum suffers from the intermittent emission.

According to the previous analysis, we have to eliminate those disturbance terms in $J(\boldsymbol{p})$ to acquire a robust location MVDR spectrum correctly. As a consequence, We propose an iterative method based on K-means clustering algorithm [17], [18] to estimate the state vector $\{\boldsymbol{b}_q\}_{q=1}^Q$ and the sources locations $\{\boldsymbol{p}_q\}_{q=1}^Q$ alternately.

The K-means clustering algorithm initializes K different clustering centers $\{\mu_k\}_{k=1}^K$ and then iterates the following two steps until convergence: step 1, every training sample is allotted into the i-th cluster represented by the nearest clustering center μ_i; step 2, every clustering center is updated with the average of all training samples in the cluster [18].

In general, only the peaks corresponding to sources which emit in the most slots appear on the original spectrum (17). The other sources emitting in less slots can be drown out in noise. In order to estimate the source positions and the number of sources, we modify the location spectrum to make all sources appear initially,

$$\hat{\boldsymbol{p}}_q^{(0)} = arg\max_{\boldsymbol{p}} J^{(0)}(\boldsymbol{p}) \quad q = 1, \ldots, \hat{Q}$$
$$J^{(0)}(\boldsymbol{p}) = \frac{1}{\sum_{i=1}^{I^{(0)}} g_i^{-1}(\boldsymbol{p})} \tag{18}$$

where

$$(g_1(\boldsymbol{p}), \ldots, g_K(\boldsymbol{p})) \triangleq \text{descend}[J_1(\boldsymbol{p}), \ldots, J_K(\boldsymbol{p})]$$

descend[·] is the descending sort operator. $\hat{Q}$ is corresponding to the number of spectrum peaks. I is the number of emitting slots and usually initialized (such as $I^{(0)} = 2, 3$) to guarantee the uniqueness of the location estimation and remove the noise spectrum values as much as possible. Obviously, if there are more than $I^{(0)}$ emitting slots (in general situations), the object function (17) is over modified initially. Though all sources appear on the over modified spectrum, we have to estimate a new I to improve the object function for better localization accuracy and resolution.

For the q-th source, we allot K MVDR-spectrum value $\{J_k(\hat{\boldsymbol{p}}_q)\}_{k=1}^K$ into two clusters (larger and smaller) using the classical K-means clustering algorithm. Note that the clustering is not required for the source emitting over all observation slots. We can identify this kind of source based on the condition of detecting sources with intermittent emission,

$$\rho \triangleq \frac{\mu_l - \mu_s}{\mu_l} > \eta \tag{19}$$

where μ_l is the clustering center of the larger cluster and μ_s is the smaller one. The condition for sources with intermittent emission (19) is based on the fact that the ratio ρ of the difference between the two clustering centers to the larger centers approaches 1 as SNR increases.

If the condition (19) is true (the source emits intermittently), the I^* is updated with the number of members in larger cluster N_l. A new object function is modified by I^*. And then the position estimation is updated based on the new object function $J^*(\boldsymbol{p})$. If the condition (19) is false (the source emits continuously), then the final sources locations will be estimated from the original spectrum (17). The whole iterative algorithm is concluded in Algorithm 1.

Algorithm 1 The Robust MVDR-DDPD Algorithm

Input: the inverse of sample correlation matrix $\{\hat{\boldsymbol{R}}_k^{-1}\}_{k=1}^K$ in (15);
the initial number of emitting slots $I^{(0)}$;
the maximum iterations M_{Iter};
the condition threshold η;
Output: the source locations estimation $\{\hat{\boldsymbol{p}}_q^*\}_{q=1}^{\hat{Q}}$.
Initial $\{\hat{\boldsymbol{p}}_q^{(0)}\}_{q=1}^{\hat{Q}}$ using (18) with $I^{(0)}$;
for q 1 *to* $\hat{Q}$ **do**
  Evaluate two clustering centers at $\hat{\boldsymbol{p}}_q^{(0)}$:
  $[\mu_l, \mu_s]$=K-means$[J_1(\hat{\boldsymbol{p}}_q^{(0)}), \ldots, J_K(\hat{\boldsymbol{p}}_q^{(0)})]$;
  if $(\mu_l - \mu_s)/\mu_l > \eta$ **then**
    while $\hat{\boldsymbol{p}}_q^* \neq \hat{\boldsymbol{p}}_q$ *and iterations* $\leq M_{Iter}$ **do**
      Evaluate the number of members in the larger cluster:
      N_l=K-means$[J_1(\hat{\boldsymbol{p}}_q), \ldots, J_K(\hat{\boldsymbol{p}}_q)]$;
      Update the number of emitting slots:
      $I^* = N_l$;
      Update the location estimation $\hat{\boldsymbol{p}}_q^*$ using (18) with I^*.
    end
  else
    Update the location estimation $\hat{\boldsymbol{p}}_q^*$ using (12).
  end
end

It's worth pointing out that the proposed algorithm hardly need to tune predefined parameters using computer simulations, for we use the K-means clustering algorithm which is based on the data to estimate the number of emitting slots adaptively, instead of using an absolute threshold. The only threshold used to detect the intermittent emission case η is usually selected between [0.2, 0.3] since it is compared with the relative difference between the two clustering centers.

IV. SIMULATION RESULTS AND DISCUSSION

In this section, we design several numerical simulations to verify and evaluate the performance of the proposed method, denoted by Modified-MVDR-DPD, and compare it with the estimator based on alternative projection technique and the original Capon-type estimator [9], denoted by AP-DPD and Capon-DPD respectively, and the Cramer-Rao lower bound (CRLB), detailed in [9].

The iterative AP-DPD estimator is given as

$$\hat{\boldsymbol{p}}_q^{i+1} = arg \max_{\boldsymbol{p}} \sum_{k=1}^{K} \frac{\boldsymbol{w}_k^H(\boldsymbol{p}, \hat{\boldsymbol{\xi}}_{\neg q}^i)\hat{\boldsymbol{R}}_k \boldsymbol{w}_k(\boldsymbol{p}, \hat{\boldsymbol{\xi}}_{\neg q}^i)}{\boldsymbol{w}_k^H(\boldsymbol{p}, \hat{\boldsymbol{\xi}}_{\neg q}^i)\boldsymbol{w}_k(\boldsymbol{p}, \hat{\boldsymbol{\xi}}_{\neg q}^i)}$$
$$s.t.\ \boldsymbol{w}_k(\boldsymbol{p}, \hat{\boldsymbol{\xi}}_{\neg q}^i) = \boldsymbol{P}^{\perp}_{\boldsymbol{A}_k(\hat{\boldsymbol{\xi}}_{\neg q}^i)} \boldsymbol{a}_k(\boldsymbol{p}) \tag{20}$$

where $\hat{\boldsymbol{\xi}}_{\neg q}^i$ denotes the estimation of all sources positions except q-th source position $\hat{\boldsymbol{p}}_q^i$ at i-th iteration and

$$\boldsymbol{P}^{\perp}_{\boldsymbol{A}_k(\hat{\boldsymbol{\xi}}_{\neg q}^i)} \triangleq \boldsymbol{I}_M - \boldsymbol{A}_k(\hat{\boldsymbol{\xi}}_{\neg q}^i)[\boldsymbol{A}_k^H(\hat{\boldsymbol{\xi}}_{\neg q}^i)\boldsymbol{A}_k(\hat{\boldsymbol{\xi}}_{\neg q}^i)]^{-1}\boldsymbol{A}_k^H(\hat{\boldsymbol{\xi}}_{\neg q}^i)$$
$$\boldsymbol{A}_k(\hat{\boldsymbol{\xi}}_{\neg q}^i) \triangleq [\boldsymbol{a}_k(\hat{\boldsymbol{p}}_1^i), \ldots, \boldsymbol{a}_k(\hat{\boldsymbol{p}}_{q-1}^i), \boldsymbol{a}_k(\hat{\boldsymbol{p}}_{q+1}^i), \ldots, \boldsymbol{a}_k(\hat{\boldsymbol{p}}_Q^i)]$$

The AP-DPD estimator is dependent on the performance of the model order determination since the optimization problem (20) is solved with the prior knowledge of the number of sources, while the prior knowledge is not required for application of MVDR on which the proposed method is based. Furthermore, the estimation of other sources positions $\hat{\boldsymbol{\xi}}_{\neg q}$ is required to solve the optimization problem (20) about the q-th source position $\hat{\boldsymbol{p}}_q$. As a consequence, all position estimators influences one another, while there is no such dependence among the proposed estimators in (18), for the multiple-sources localization problem was decoupled into several independent single source localization problems which can be solved in parallel.

Considering that the MVDR based DPD estimator can be biased when there exists more than one source in the scenario [19], we don't only focus on the RMSE but also the bias error (BE),

$$RMSE = \sqrt{\frac{1}{N_{sim}} \sum_{s=1}^{N_{sim}} \|\hat{\boldsymbol{p}}(s) - \boldsymbol{p}\|_2^2} \tag{21}$$

$$BE = \|\frac{\sum_{s=1}^{N_{sim}} \hat{\boldsymbol{p}}(s)}{N_{sim}} - \boldsymbol{p}\|_2 \tag{22}$$

where N_{sim} is the number of Monte carlo simulations and we used $N_{sim} = 2000$ to obtain statistical results. $\hat{\boldsymbol{p}}(s)$ is the position estimation of the s-th simulation. As illustrated in Fig.2 and Fig.3a, we consider the scenario in which a uniform circular array (UCA) with $M = 10$ elements at

$$\boldsymbol{d}_m = \frac{\lambda}{2}(sin\frac{\pi}{M})^{-1}(cos\frac{2m\pi}{M}, sin\frac{2m\pi}{M}, 0)^T \tag{23}$$

where $\frac{\lambda}{2}(sin\frac{\pi}{M})^{-1}$ is the radius of the UCA. It moves along an arc from $(-500, -500, 500)^T$m to $(500, -500, 500)^T$m at a speed of 200m/s. the received signals are sampled at

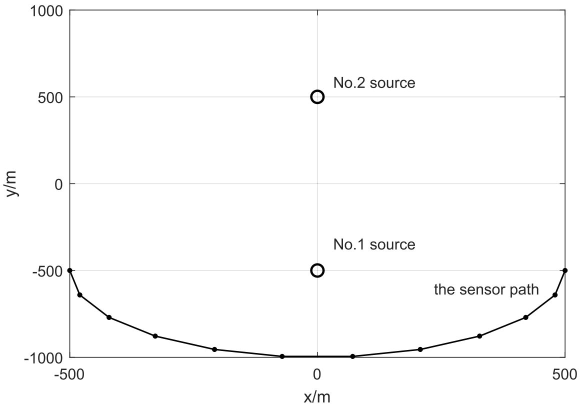

FIGURE 2. **The problem geometry with sources positions $p_1 = (0, -500, 0)^T$ m, $p_2 = (0, 500, 0)^T$ m and emitting probabilities $P_{k,1} = 1, P_{k,2} = 0.7$.**

$K = 12$ positions which are distributed on the arc uniformly. The sampling period is 0.05ms and there are $N = 100$ samples per batch. The carrier frequency of the received signals is $f_c = 200$MHz ($\lambda = c/f_c = 1.5$m, $c = 3 \times 10^8$ m/s).

Two ground sources are located at positions $\boldsymbol{p}_1, \boldsymbol{p}_2$ and the constant emitting probabilities of the two sources are P_1, P_2. It is assumed that the emitted waveforms of each source have constant amplitude at all sensor positions $|s_{k,n,q}| = s$ and the phase of them are selected at random from a uniform distribution over $[0, 2\pi]$. Thus, the SNR is defined as that of single source signal to single element noise, SNR $= s^2/\sigma_w^2$.

The number of emitting slots of each source can be initialized to $I^{(0)} = 4$ because it is scarcely possible to be less than four when the total number of slots $K = 12$ and the emitting probability $P_q \geq 0.7$ [9]. Note that the emitting probability is not a prior knowledge so we generally choose $I^{(0)} = 2$ in practice. The threshold η used to detect intermittent emission case takes a common value 0.3. The parameters keep the same in this section unless they are mentioned specially. In our simulations, we use the simplex method of Nelder and mead [20] to find the maximum of both object function of (18) and (20). The initialization problem of AP-DPD is solved by (18) with the equal $I^{(0)}$.

First of all, we put the two sources close to each other (Fig.3a) to display the higher resolution of the modified MVDR-DPD estimator than that of the single Maximum Likelihood (SML) estimator [21],

$$\hat{\boldsymbol{p}} = arg \max_{\boldsymbol{p}} J_s(\boldsymbol{p})$$

$$J_s(\boldsymbol{p}) = \sum_{k=1}^{K} \boldsymbol{a}_k^H(\boldsymbol{p})\hat{\boldsymbol{R}}_k \boldsymbol{a}_k(\boldsymbol{p}) \tag{24}$$

The emitting probabilities $P_1 = P_2 = 0.7$ and SNR=5dB. Fig.3c-3f are the MVDR-spectrum with different I during the iteration. In the original spectrum (Fig.3c), it can be seen that the peak around No.2 source is biased and not sharp while there is no peak around No.1 source. Both of accuracy and resolution are degraded by the missing emission. Fig.3d shows that there are two irregular peaks on the initial spectrum which removes the effect of intermittent emission and make the peaks of the two sources appear. Fig.3e and Fig.3f display the modified spectrum for two sources respectively. Compared to the SML spectrum (Fig.3b) on which there is only one biased peak, the modified spectrums have accurate and sharp peaks around the two sources. The proposed estimator acquires both higher accuracy and resolution.

Theoretically, the statistical performance of the proposed method is determined by the accuracy rate of estimating the number of emitting slots and the ability of detecting the intermittent emission case. Therefore, our simulations are focus on the performance in these two aspects.

In order to display the performance of the proposed method for the two sources clearly, we put them at $\boldsymbol{p}_1 = (0, -500, 0)^T$ m, $\boldsymbol{p}_2 = (0, 500, 0)^T$ m (Fig.2), i.e. one source is close to the sensor and the other is far away from the sensor. The emitting probabilities is set as $P_1 = 1$ (continuous emission),$P_2 = 0.7$ (intermittent emission). We start with varying the SNR between -20 dB and 10 dB to evaluate the effect of SNR on the accuracy rate of estimating the number of emitting slots and their attributes on the performance of the proposed method.

Table 2 shows that the accuracy rate of estimating the number of emitting slots increases with SNR, which makes the asymptotic performance of the proposed algorithm expected.

TABLE 2. **Accuracy rate VS SNR.**

SNR/dB	-20	-15	-10	-5	0	5	10
Accuracy/%	1.5	1.5	50.8	96.2	99.90	99.95	100

Fig.4 shows that the square-root of CRLB and the RMSE of three algorithms for the two sources respectively. The RMSE for the No.2 source of the proposed algorithm (the solid red triangle line) is lower than that of the estimator based on the original Capon-type object function (the dashed green triangle line), which indicates that the Capon-type object function suffers from the intermittent emission while the proposed method is more robust. Besides, the similar two RMSE lines for the No.1 source at $(0, -500, 0)^T$ m (the red and green square lines) coincide with each other, which indicates that the proposed method to modify the original object function doesn't degrade the performance of localizing the source with continuous emission since the false alarm probability of detecting the intermittent emission case is zero.

The RMSE of the proposed method for the two sources (the two red lines) almost coincide with that of AP-DPD (the two blue lines) respectively. All of them approximate the CRLB as the SNR increases, which indicates that both of the two methods have similarly asymptotic performance. The similarly asymptotic performance is expected since the optimization problem (20), which is derived from the ML estimation, can be interpreted as a conventional beamformer in direction $\boldsymbol{p}$ with deterministic nulling of sources at locations $\hat{\boldsymbol{\xi}}_{\neg q}^{i}$ [9]

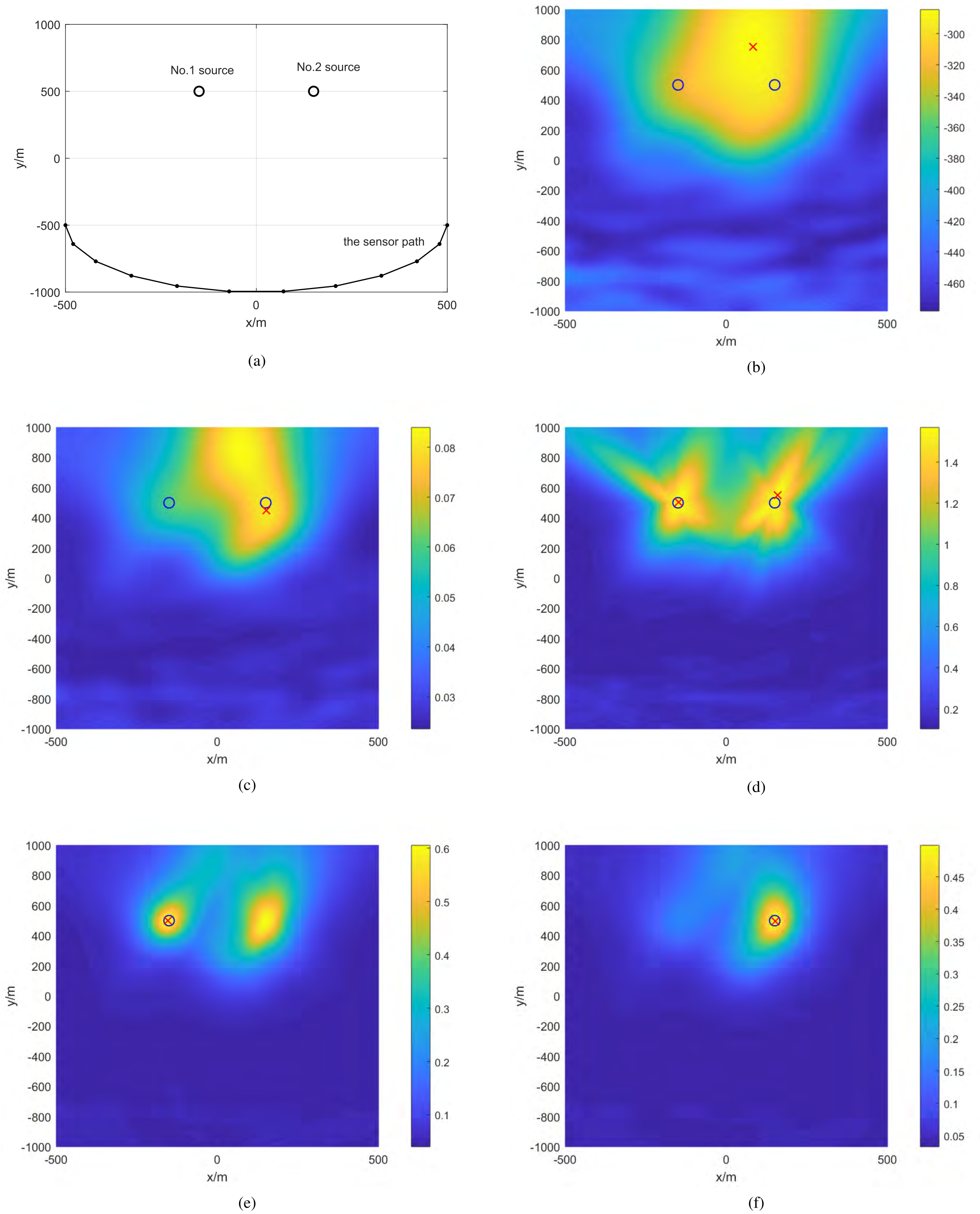

FIGURE 3. **The MVDR-spectrum with true positions (circles) and estimated positions(crosses), $P_1 = P_2 = 0.7$ and SNR = 5dB. (a) The single Maximum Likelihood spectrum. (b) The original spectrum, $I = 12$. (c) The modified spectrum of the No.1 source, $I^* = 7$. (d) The modified spectrum of the No.2 source, $I^* = 9$.**

while the proposed optimization problem (9) can be interpreted as an adaptive MVDR-beamformer in direction $\boldsymbol{p}$ with adaptive nulling, which explains the independence among the proposed estimators in (18).

Fig.5 shows the bias error of three algorithms respectively. It can be seen that the three estimators for the No.1 source are all nearly unbiased. For the No.2 source, the AP-DPD is also unbiased (the bias errors at SNR $= -20, -15$dB result

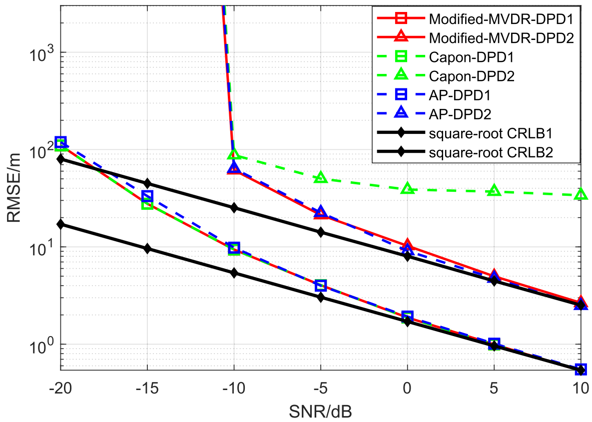

FIGURE 4. RMSE vs. SNR, the square marks for the No.1 source at $(0, -500, 0)^T$ m and the triangle marks for the No.2 source at $(0, 500, 0)^T$ m.

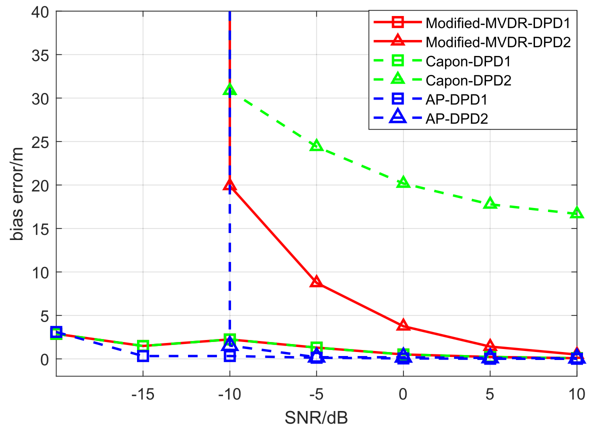

FIGURE 5. Bias error vs. SNR, the square marks for the No.1 source at $(0, -500, 0)^T$ m and the triangle marks for the No.2 source at $(0, 500, 0)^T$ m.

from the invalid position initialization) and the bias error of the proposed estimator (18) converges to zero with SNR (asymptotically unbiased) while the original Capon-DPD are biased because of the missing emission.

Next, we evaluate the effect of the sensor height $\boldsymbol{u}(3)$ on the accuracy rate of estimating the number of emitting slots and their contribution to the performance of the proposed method. Note that if the sensor and the two sources are collinear in earth-fixed coordinates, it's likely to over-estimate the number of emitting slots since their spatial signature is DOA in our problem formulation (2).

To be specific, the two sources have similar array transfer vector when the sensor (assume $\boldsymbol{u}(3) = 0$m) is close to the y-axis of the earth-fixed coordinates (i.e. the sixth and seventh locations of the sensor path in Fig.2). On account of the similar array transfer vector, it's impossible to generate nulling of No.1 source when we estimate the No.2 source position using (18). It means that, regardless of whether the No.2 source emits at sixth and seventh slots or not, $J_6(\hat{\boldsymbol{p}}_2)$, $J_7(\hat{\boldsymbol{p}}_2)$ will be large when the No.1 source emits (it's true in our scenario).

In order to verify the previous theoretical conclusion, we make the No.2 source idle from fifth to eighth slots and increase $\boldsymbol{u}(3)$ from 0 to 300m (SNR = 0dB).

In table 3, it can be seen that the accuracy rate of estimating the number of emitting slots of the No.2 source becomes very low (4.3%) when the sensor is located on the land (i.e $\boldsymbol{u}(3)$=0m) and increases to 100% as $\boldsymbol{u}(3) = 300m$,for the sensor and the two sources are no longer collinear. The essential reason of the results is that the linear correlation of the spatial signature such as DOA, TOA and DFS is damaged.

TABLE 3. Accuracy rate VS the sensor height.

$\boldsymbol{u}(3)$/m	0	50	100	150	200	250	300
Accuracy/%	4.3	3.9	4.6	15	66.5	98.7	100

Fig.6 displays the square-root CRLB and the RMSE of the proposed method and original Capon-DPD. Note that the RMSE of the Modified-MVDR-DPD for the No.2 source (the solid red triangle line) decreases with the sensor height $\boldsymbol{u}(3)$ and approaches the square-root CRLB at $\boldsymbol{u}(3) = 250, 300$m while that of the Capon-DPD (the dashed green triangle line) is always higher even though $\boldsymbol{u}(3)$ is up to 300m. It indicates that the Capon-type object function suffers from the intermittent emission while the robustness to the intermittent emission of the proposed method is enhanced. Besides, the similar two RMSE lines for the No.1 source (the two square lines) coincide with each other, which indicates that the proposed method to improve the original object function don't degrade the performance of localizing the source with continuous emission, for the false alarm probability of detecting the intermittent emission case is zero.

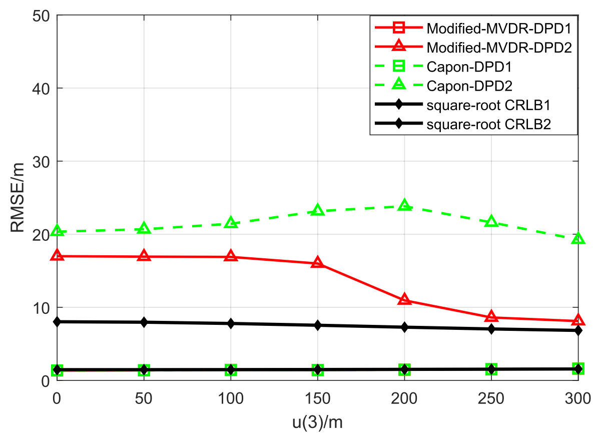

FIGURE 6. RMSE vs. the sensor height, the square marks for the No.1 source at $(0, -500, 0)^T$ m and the triangle marks for the No.2 source at $(0, 500, 0)^T$ m.

Fig.7 shows the bias error of Modified-MVDR-DPD and Capon-DPD respectively. The estimators for the No.1 source of two methods are all near unbiased. For the No.2 source, the bias error of the Modified-MVDR-DPD is improved obviously at $\boldsymbol{u}(3) = 200$m since the accuracy rate

TABLE 4. **The ROC of detecting the intermittent emission case in geometry Fig.2.**

	η	0	0.1	0.2	0.3	0.4	0.5	0.6	0.7	0.8	0.9	1
$\hat{P}_d$	-10dB	1.00	1.00	0.98	0.70	0.07	0	0	0	0	0	0
	0dB	1.00	1.00	0.99	0.99	0.99	0.99	1.00	1.00	0.97	0	0
	10dB	1.00	1.00	1.00	0.99	0.99	0.99	0.97	1.00	1.00	0.98	0
$\hat{P}_f$	-10dB	1.00	0.98	0.15	0.01	0	0	0	0	0	0	0
	0dB	1.00	0.58	0.01	0	0	0	0	0	0	0	0
	10dB	1.00	0.01	0	0	0	0	0	0	0	0	0

TABLE 5. **The ROC of detecting the intermittent emission case in geometry Fig.3a.**

	η	0	0.1	0.2	0.3	0.4	0.5	0.6	0.7	0.8	0.9	1
$\hat{P}_d$	-10dB	1.000	1.000	0.852	0.384	0.028	0	0	0	0	0	0
	0dB	1.000	1.000	0.992	0.986	0.988	0.984	0.976	0.978	0.850	0	0
	10dB	1.000	0.984	0.984	0.990	0.970	0.992	0.968	0.992	0.986	0.984	0
$\hat{P}_f$	-10dB	1.000	0.988	0.456	0.104	0.010	0	0	0	0	0	0
	0dB	1.000	0.854	0.224	0.070	0.034	0.012	0.002	0.004	0	0	0
	10dB	1.000	0.164	0.016	0.004	0	0	0	0	0	0	0

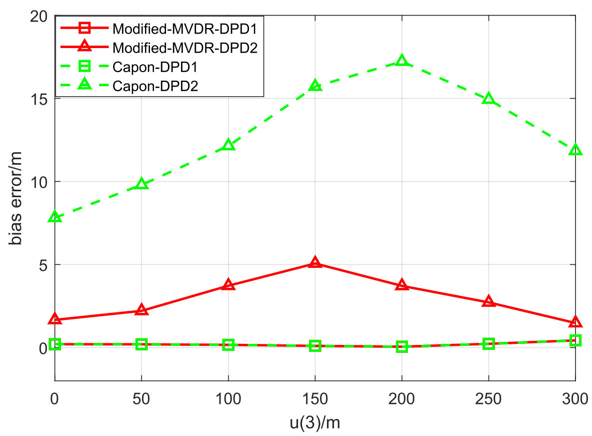

FIGURE 7. **Bias error vs. the sensor height, the square marks for the No.1 source at $(0, -500, 0)^T$ m and the triangle marks for the No.2 source at $(0, 500, 0)^T$ m.**

approaches 100% and the two sources can be distinguished at this sensor height.

Finally, we vary the threshold η from 0 to 1 to evaluate the Receiver Operating Characteristic (ROC) of detecting the intermittent emission case using the statistic ρ in (19). The detection probability $\hat{P}_d$ and the false alarm probability $\hat{P}_f$ are estimated over N_{sim}=500 simulations at SNR $= -10, 0, 10$dB respectively. Table 4 and Table 5 show the ROC of the statistic ρ under two different geometries respectively. It can be seen that the ROC of ρ is almost perfect (i.e. $\hat{P}_d$ approaches 1 and $\hat{P}_f$ approaches 0 even though the threshold η vary between a wide range [0.2,0.8] in Table 4 and [0.3,0.7] in Table 5) at higher SNR $= 0, 10$dB. The sources with intermittent emission can be identified easily and correctly. However, it is needed to make a trade-off between $\hat{P}_d$ (the higher $\hat{P}_d$ benefits the localization of sources with intermittent emission) and $\hat{P}_f$ (the lower $\hat{P}_f$ benefits the localization of sources with continuous emission) in the case of low SNR $= -10$dB. In geometry Fig.3a (the distance between the two sources is up to 1km), $\eta = [0.2, 0.3]$ is a good trade-off at SNR $= -10$dB. While there is no satisfying choice of η in geometry Fig.3a (the distance between the two sources is only 0.3km).

According to the simulation results, we can conclude that the ROC of the proposed statistic ρ gets better as the separability of sources is enhanced.

V. CONCLUSION

We research to estimate the positions and total number of multiple sources with intermittent emission using the received signals intercepted by a moving antenna array at multiple observation slots. We combine the DPD concept and the MVDR criterion to design an clustering based adaptive algorithm to solve the DDPD problem. The algorithm doesn't rely on the model order determination and solves the DDPD problem without the prior knowledge of the effective number of sources. it decouples the multiple-sources localization problem into several independent single source localization problems which can be solved in parallel. It can be seen that the algorithm gets high resolution and asymptotic performance of localization in simulation section. Note that the idea of combining DPD and MVDR to localize the emitter with missing emission can be generalized to localize the frequency-hopping emitters or the emitters whose signals are only intercepted by a part of receivers. Both of the two kinds of emitters are common in practice. The related research work is underway.

ACKNOWLEDGMENT

The authors would like to thank the anonymous reviewers for providing valuable comments and suggestions that have helped improving the quality of the paper. And thanks are due to Dr. Qun Wan for the constructive suggestions and valuable discussions.

REFERENCES

[1] Y. Zou and Q. Wan, "Asynchronous time-of-arrival-based source localization with sensor position uncertainties," *IEEE Commun. Lett.*, vol. 20, no. 9, pp. 1860–1863, Sep. 2016.
[2] Y. Zou, H. Liu, X. Wei, and Q. Wan, "Semidefinite programming methods for alleviating sensor position error in TDOA localization," *IEEE Access*, vol. 5, pp. 23111–23120, 2017.
[3] Y. Zou, H. Liu, and Q. Wan, "Joint synchronization and localization in wireless sensor networks using semidefinite programming," *IEEE Internet Things J.*, vol. 5, no. 1, pp. 199–205, Feb. 2018.
[4] Y. Sun, K. C. Ho, and Q. Wan, "Solution and analysis of TDOA localization of a near or distant source in closed form," *IEEE Trans. Signal Process.*, vol. 67, no. 2, pp. 320–335, Jan. 2019.
[5] Y. Sun and Q. Wan, "Position determination for moving transmitter using single station," *IEEE Access*, vol. 6, pp. 61103–61116, 2018.
[6] A. J. Weiss, "Direct position determination of narrowband radio frequency transmitters," *IEEE Signal Process. Lett.*, vol. 11, no. 5, pp. 513–516, May 2004.
[7] A. Weiss, "Direct geolocation of wideband emitters based on delay and Doppler," *IEEE Trans. Signal Process.*, vol. 59, no. 6, pp. 2513–2521, Jun. 2011.
[8] S. S. Blackman, "Multiple hypothesis tracking for multiple target tracking," *IEEE Aerosp. Electron. Syst. Mag.*, vol. 19, no. 1, pp. 5–18, Jan. 2004.
[9] M. Oispuu and U. Nickel, "Direct detection and position determination of multiple sources with intermittent emission," *Signal Process.*, vol. 90, no. 12, pp. 3056–3064, Dec. 2010.
[10] I. Ziskind and M. Wax, "Maximum likelihood localization of multiple sources by alternating projection," *IEEE Trans. Acoust., Speech Signal Process.*, vol. 36, no. 10, pp. 1553–1560, Oct. 1988.
[11] J. Capon, "High-resolution frequency-wavenumber spectrum analysis," *Proc. IEEE*, vol. 57, no. 8, pp. 1408–1418, Aug. 1969.
[12] T. Tirer and A. J. Weiss, "High resolution direct position determination of radio frequency sources," *IEEE Signal Process. Lett.*, vol. 23, no. 2, pp. 192–196, Feb. 2015.
[13] L. Tzafri and A. J. Weiss, "High-resolution direct position determination using MVDR," *IEEE Trans. Wireless Commun.*, vol. 15, no. 9, pp. 6449–6461, Sep. 2016.
[14] T. Tirer and A. J. Weiss, "High resolution localization of narrowband radio emitters based on Doppler frequency shifts," *Signal Process.*, vol. 141, pp. 288–298, Dec. 2017.
[15] M. Hawkes and A. Nehorai, "Acoustic vector-sensor beamforming and capon direction estimation," *IEEE Trans. Signal Process.*, vol. 46, no. 9, pp. 2291–2304, Sep. 1998.
[16] D. H. Brandwood, "A complex gradient operator and its applica-tion in adaptive array theory," *IEE Proc. F, Commun., Radar Signal Process.*, vol. 130, no. 1, pp. 11–16, Feb. 2008.
[17] P. Angelov, *Fundamentals of Machine Learning and Pattern Recognition*. Hoboken, NJ, USA: Wiley, 2012.
[18] Y. Bengio and A. Courville, *Deep Learning of Representations*. Berlin, Germany: Springer, 2013.
[19] T. Tirer and A. J. Weiss, "Performance analysis of high resolution direct position determination method," *IEEE Trans. Signal Process.*, vol. 65, no. 3, pp. 544–554, May 2016.
[20] J. A. Nelder and R. Mead, "A simplex method for function minimization," *Comput. J.*, vol. 7, no. 4, pp. 308–313, 1965.
[21] A. Amar and A. J. Weiss, *Localization of Narrowband Radio Emitters Based on Doppler Frequency shifts*. Piscataway, NJ, USA: IEEE Press, 2008.

KEGANG HAO (S'17) was born in 1993. He received the B.S. degree from the School of Electronic Engineering, University of Electronic Science and Technology of China (UESTC), Chengdu, China, in 2016, where he is currently pursuing the Ph.D. degree in information and communication engineering. His research interests include passive localization, direct position determination, array processing, and machine learning.

QUN WAN (M'04) received the B.Sc. degree in electronics engineering from Nanjing University, in 1993, and the M.Sc. and Ph.D. degrees in electronic engineering from the University of Electronic Science and Technology of China (UESTC), in 1996 and 2001, respectively, where he has been a Professor with the Department of Electronic Engineering, since 2004. From 2001 to 2003, he was a Postdoctoral with the Department of Electronic Engineering, Tsinghua University. He is currently the Director of Joint Research Lab of Array Signal Processing and the Associate Dean of the School of Electronic Engineering. His research interests include direction finding, radio localization, and signal processing based on information criterion.